

UC Irvine

UC Irvine Previously Published Works

Title

Measurement of single and double radiative low-Q2 Bhabha scattering at $E_{c.m.}=29$ GeV

Permalink

<https://escholarship.org/uc/item/1448k4dz>

Journal

Physical Review D, 39(7)

ISSN

2470-0010

Authors

Karlen, D
Abrams, G
Amidei, D
[et al.](#)

Publication Date

1989-04-01

DOI

10.1103/physrevd.39.1861

Copyright Information

This work is made available under the terms of a Creative Commons Attribution License, available at <https://creativecommons.org/licenses/by/4.0/>

Peer reviewed

Measurement of single and double radiative low- Q^2 Bhabha scattering at $E_{c.m.} = 29$ GeV

D. Karlen, ^{α ,^(a)} G. Abrams, ^{β} D. Amidei, ^{β ,^(b)} A. R. Baden, ^{β ,^(c)} T. Barklow, ^{α} A. M. Boyarski, ^{α}
 J. Boyer, ^{β} P. R. Burchat, ^{α ,^(d)} D. L. Burke, ^{α} F. Butler, ^{β} J. M. Dorfan, ^{α} G. J. Feldman, ^{α}
 G. Gidal, ^{β} L. Gladney, ^{α ,^(e)} M. S. Gold, ^{β} G. Goldhaber, ^{β} L. Golding, ^{β ,^(f)} J. Haggerty, ^{β ,^(g)}
 G. Hanson, ^{α} K. Hayes, ^{α} D. Herrup, ^{β ,^(h)} R. J. Hollebeek, ^{α ,^(e)} W. R. Innes, ^{α} J. A. Jaros, ^{α}
 I. Juricic, ^{β ,⁽ⁱ⁾} J. A. Kadyk, ^{β} S. R. Klein, ^{α} A. J. Lankford, ^{α} R. R. Larsen, ^{α} B. W. LeClaire, ^{α ,^(j)}
 M. Levi, ^{γ} N. S. Lockyer, ^{α ,^(e)} V. Lüth, ^{α} M. E. Nelson, ^{β ,^(k)} R. A. Ong, ^{α ,^(b)} M. L. Perl, ^{α}
 B. Richter, ^{α} K. Riles, ^{α} P. C. Rowson, ^{β ,⁽ⁱ⁾} T. Schaad, ^{γ ,^(l)} H. Schellman, ^{β ,^(b)} W. B. Schmidke, ^{β}
 P. D. Sheldon, ^{β ,^(m)} G. H. Trilling, ^{β} D. R. Wood, ^{β ,⁽ⁿ⁾} and J. M. Yelton, ^{α ,^(o)}

^{α} Stanford Linear Accelerator Center, Stanford University, Stanford, California 94305

^{β} Lawrence Berkeley Laboratory and Department of Physics, University of California, Berkeley, California 94720

^{γ} Department of Physics, Harvard University, Cambridge, Massachusetts 02138

(Received 26 August 1988)

The process $e^+e^- \rightarrow e^+e^-\gamma(\gamma)$, where one electron scatters at a small angle, is studied with data from the Mark II detector at the SLAC storage ring PEP. The data are in excellent agreement with a Monte Carlo calculation and include a large contribution from order α^4 . The ratio of measured to calculated cross sections is $R = 0.993 \pm 0.017 \pm 0.015$, where the first error is statistical and the second systematic. This is a sensitive test of the calculation of the dominant background for neutrino-counting experiments.

We use data from the Mark II detector, taken during its operation at the SLAC e^+e^- storage ring PEP, to study inelastic electron-positron scattering where only one electron and one or two high-energy photons are observed at large angles. The other electron involved in the interaction goes undetected or is detected at a small angle. The process is dominated by the exchange of a nearly real photon between the electron and positron.

The motivation for this work is to test a recent calculation¹ that includes the dominant QED radiative correction to low- Q^2 radiative Bhabha scattering. A good understanding of this process is important because it is the largest background to experiments that determine the number of light neutrino species and search for other neutral weakly interacting particles, by studying the reaction²

$$e^+e^- \rightarrow \gamma + \text{unobserved particles}.$$

The elements of the Mark II detector³ crucial to this study are the cylindrical vertex and main drift chambers and the liquid-argon calorimeter. The drift chambers provide charged-particle tracking with 23 layers of cells from a radius of 10–145 cm from the interaction point. By measuring track curvature due to the axial magnetic field of 2.3 kG provided by a surrounding solenoid coil, the chambers determine particle momenta with a resolution $(\delta p/p)^2 = (0.02)^2 + (0.01p_1)^2$ where p_1 is the transverse momentum in GeV/c. The calorimeter consists of eight planar modules that surround the coil, each made of over 14 radiation lengths of lead-liquid-argon sandwich, giving an energy resolution of $0.15\sqrt{E}$ (E in GeV). The active region of the calorimeter, roughly $|\cos\theta| < 0.66$, defines the fiducial volume of the detector for the analyses described below.

Before presenting the analysis of low- Q^2 radiative Bhabha scattering, we describe a measurement of the integrated luminosity using wide-angle Bhabha-scattering events. For these events, the Mark II detector typically makes four independent measurements: the two electron tracks (each with momentum 14.5 GeV/c) reconstructed in the drift chambers and the two electromagnetic showers (with energy 14.5 GeV) reconstructed in the liquid-argon calorimeter. High efficiency is obtained by requiring at least three of these tracks and showers to be reconstructed in the fiducial volume with momentum (energy) above 5 GeV/c (5 GeV). To eliminate the background from cosmic rays, events with only a single shower above threshold are required to have both track flight times to the outer radius of the drift chambers within 2 ns of the expected values. Events with only one charged track above threshold are required to have a minimum number of drift-chamber layers with a signal along each shower direction. This reduces the background from two-photon annihilation, $e^+e^- \rightarrow \gamma\gamma$ where a photon converts in the detector material, and from low- Q^2 radiative Bhabha scattering. The background from τ pair production is suppressed by requiring at least one shower to have more than 10 GeV.

The Monte Carlo event generator of Berends and Kleiss,⁴ along with the detector simulation program, is used to integrate the Bhabha cross section over the experimental acceptance. The acollinearity angle distributions of the data and Monte Carlo samples are in good agreement. When only one track is reconstructed with momentum above threshold, the acollinearity angle is determined using the shower position. For this analysis, the acollinearity angle is required to be less than 400 mrad.

Corrections to the measurement due to backgrounds, dominated by τ pair production, and inefficiencies not included in the detector simulation, are each less than 0.2%. The dominant systematic uncertainty is in the scale of the $\cos\theta$ measurements and the error is determined to be $(0.2 \pm 1.2)\%$, using the observed angular distribution of the Bhabha events. An uncertainty of 0.5% is assigned to the calculation of the Bhabha-scattering cross section. The integrated luminosity of the data set is $209.2 \pm 0.5 \pm 2.9 \text{ pb}^{-1}$, where the first error is statistical and the second is systematic.

For the analysis of low- Q^2 radiative Bhabha scattering, an electron and photon are required to be in the fiducial volume, each with more than 2 GeV energy as measured by the liquid-argon calorimeter. Events with a second photon of energy greater than 300 MeV and isolated by at least 30 cm in the calorimeter from any other shower are treated in a separate analysis, described later. The primary backgrounds are from two-photon annihilation where one photon converts in the beam pipe or drift chamber, and from wide-angle Bhabha scattering where only one electron is reconstructed because of tracking errors or hard bremsstrahlung. Events from these sources are primarily back to back; to reduce these backgrounds, the electron and photon are required to have an acollinearity angle greater than 50 mrad. The backgrounds are further reduced by requiring a minimum number of drift-chamber layers with a signal for the electron candidate, and rejecting photon candidates with too many layers. In order to select low- Q^2 events, the event plane, as determined by the electron and photon directions, must be within 50 mrad of the beam direction. A total of 3182 events pass the selection criteria.

The Monte Carlo event-generator program¹ is used to generate a sample equivalent to 10 times the data sample, with the small-angle electron scattering by less than 100 mrad, and indicates the total cross section for the acceptance described above is $14.88 \pm 0.07 \text{ pb}$. For comparison, a sample generated according to the lowest-order calculation predicts a cross section of $13.60 \pm 0.08 \text{ pb}$. The angular distributions of the wide-angle electrons and photons are in good agreement with the Monte Carlo calculation. Small-angle electrons scattered between 21 and 80 mrad are also detected and follow the Monte Carlo distributions. The sum of the wide-angle electron and photon energies are compared with order- α^3 and $-\alpha^4$ Monte Carlo predictions in Fig. 1. The low total-energy region is inaccessible to a three-body final state by momentum conservation. To better separate the three- and four-body final states, a quantity⁵ related to the missing mass $\Delta = E_{\text{miss}} - |\mathbf{p}_{\text{miss}}|$ is shown in Fig. 2. Excellent agreement between data and the Monte Carlo calculation is observed.

To estimate the number of accepted events in which the small-angle electron scatters above 100 mrad, Monte Carlo events generated according to order α^3 are used. Assuming an enhancement of $(10 \pm 5)\%$ from the next-order correction, a total of 88 ± 10 such events are expected. The Monte Carlo program is also used to generate an order- α^4 sample with the small-angle electron between 100 and 300 mrad. The calculation of the radiative

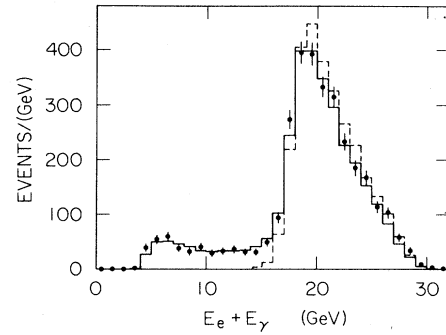


FIG. 1. The sum of the electron and photon energies in the central detector. The points show the data and the solid (dashed) histogram shows the order- α^4 ($-\alpha^3$) prediction normalized to the measured integrated luminosity.

correction may not be accurate for such large Q^2 , but the sample indicates that 93 ± 5 events would contribute. The background from two-photon annihilation where one photon converts is estimated with another Monte Carlo program⁶ to be 24 ± 5 events.

The trigger inefficiency is not included in the detector simulation, but is estimated to be only 0.25%. The drift-chamber cell-occupancy requirements also introduce a small inefficiency of 0.35%. Extra false showers that are occasionally reconstructed in the modules of the primary showers due to noise cause an inefficiency of $(0.4 \pm 0.2)\%$.

A systematic uncertainty of 0.6% arises from the simulation of a filter program which uses hardware information not generated for the Monte Carlo data sets. The uncertainty due to the association of drift-chamber tracks and liquid-argon tracks is 0.5%. The total-cross-section measurement for this process is more sensitive to a scale error in the $\cos\theta$ measurement than for Bhabha scattering. In this case the systematic error is $(0.4 \pm 2.1)\%$, as determined by an analytic integration of the lowest-order

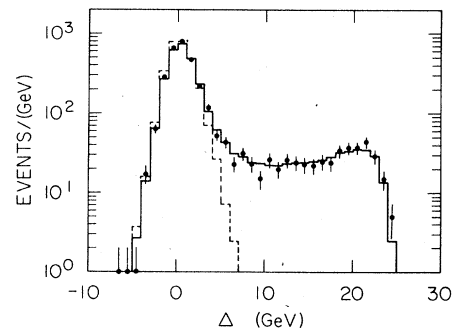


FIG. 2. The distribution for the Δ function, $\Delta = E_{\text{miss}} - |\mathbf{p}_{\text{miss}}|$. The points show the data and the solid (dashed) histogram shows the order- α^4 ($-\alpha^3$) prediction. Three-body final states have $\Delta=0$; the width of the order- α^3 distribution is due to the detector resolution.

formula. This uncertainty is partially canceled in the ratio with the integrated luminosity. An uncertainty due to a possible error in the beam center determination, is estimated to be 0.3%.

The measured cross section is $14.77 \pm 0.26 \pm 0.21$ pb, where the first error is statistical and the second systematic, and is in excellent agreement with the calculated value of 14.88 ± 0.07 pb. The ratio of measured to calculated cross sections is $R = 0.993 \pm 0.017 \pm 0.015$.

An analysis of low- Q^2 double radiative Bhabha scattering is done to further test the tree-level fourth-order calculation.¹ In addition to satisfying the selection criteria described above for the general analysis, $(e)e\gamma\gamma$ candidate events must have a second photon in the liquid-argon acceptance with a measured energy of at least 300 MeV, which is separated from any other shower by more than 30 cm. The acollinearity and event-plane angle cuts are not applied.

To suppress high- Q^2 events and other backgrounds such as false shower reconstruction, the events are required to be consistent with a four-body final state with the missing electron along the beam direction. By using the angular information alone, the energies of the three observed particles can be calculated and compared with the measured values. A simple χ^2 is calculated, assuming Gaussian momentum and energy resolution functions and ignoring the errors in the angular quantities. This χ^2 is required to be less than 36 and the recalculated energies must all be above 300 MeV. A total of 41 $(e)e\gamma\gamma$ events are selected.

The same Monte Carlo sample is used in this analysis, where the small-angle electron is constrained to be within 100 mrad of the beam direction, and predicts a total cross section of 0.188 ± 0.009 pb. The angular distributions of the electrons and photons agree with the Monte Carlo expectations. Properties of the secondary photon are shown in Fig. 3. In Fig. 3(a) the minimum azimuthal separation of the electron is given, and as expected, the majority of events have one photon close to the electron. Figure 3(b) shows the second largest photon energy, and for low energies is consistent with the expected $1/k$ distribution. Figure 4 shows the $e\gamma$, $\gamma\gamma$, and $e\gamma\gamma$ invariant-mass distributions, as calculated from the kinematically fitted energies. Again, good agreement with the Monte Carlo calculation is seen.

Few events with the small-angle electron scattered above 100 mrad are expected to pass the χ^2 requirement. Monte Carlo data with an electron scattered between 100 mrad and 300 mrad predict only 4 events to pass in a sample representing 3.5 times the integrated luminosity of the data. Electrons above 300 mrad are detected in the end-cap calorimeter, and all such events have very large χ^2 . The number of events with the small-angle electron scattered above 100 mrad is thus estimated to be 1 ± 1 . The number of background events from $e^+e^- \rightarrow \gamma\gamma\gamma$, where one of the photons converts in the detector material, is estimated to be 1 ± 1 from Monte Carlo studies.

The systematic uncertainties discussed in the previous analysis also apply here. The dominant uncertainty in this analysis is in the simulation of the χ^2 topology requirement. For low values of χ^2 the data and Monte Car-

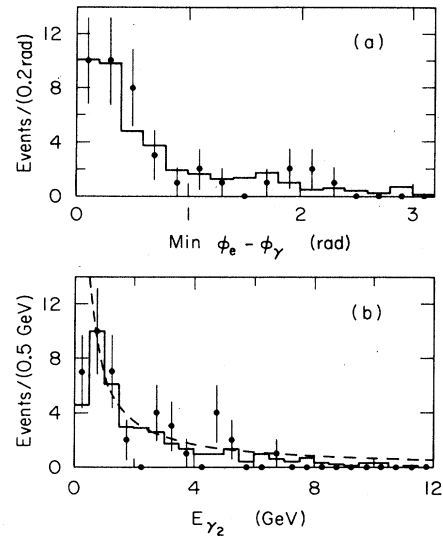


FIG. 3. Properties of the secondary photon in $(e)e\gamma\gamma$ events. The data are shown by the points, and the Monte Carlo simulation by the histograms: (a) the minimum $e\gamma$ azimuthal separation; (b) the second largest photon energy, compared to a $1/k$ distribution given by the dashed curve.

lo distributions are in good agreement. A total of 18 events fail the χ^2 cut and are not obvious backgrounds, as determined by scanning the event displays; the Monte Carlo simulation reproduces this effect and predicts 17 ± 2 events of this type. Hence, the uncertainty is taken to be the equivalent of 2 events.

The measured cross section is $0.187 \pm 0.029 \pm 0.011$ pb, where the first error is statistical and the second systematic, and is in excellent agreement with the calculated value of 0.188 ± 0.009 pb.

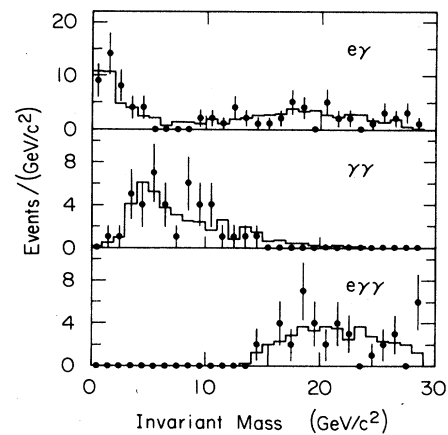


FIG. 4. The invariant-mass distributions for $(e)e\gamma\gamma$ events. The $e\gamma$ distribution has two entries per event. The data are shown by the points and the Monte Carlo simulation by the histograms.

In conclusion we have measured single and double radiative low- Q^2 Bhabha scattering and find excellent agreement with a calculation which includes the dominant part of the fourth-order QED radiative correction.

This work was supported in part by the Department of Energy under Contracts Nos. DE-AC03-76SF00515, DE-AC03-76SF00098, and DE-AC02-76ER03064.

-
- (a) Present address: Carleton University, Ottawa, Canada K1S 5B6.
- (b) Present address: University of Chicago, Chicago, IL 60637.
- (c) Present address: Harvard University, Cambridge, MA 021138.
- (d) Present address: University of California, Santa Cruz, CA 95064.
- (e) Present address: University of Pennsylvania, Philadelphia, PA 19104.
- (f) Present address: Therma-Wave Corporation, Fremont, CA 94539.
- (g) Present address: Brookhaven National Laboratory, Upton, NY 11973.
- (h) Present address: Fermi National Laboratory, Batavia, IL 60510.
- (i) Present address: Columbia University, New York, NY 10027.
- (j) Present address: University of Wisconsin, Madison, WI 53706.
- (k) Present address: California Institute of Technology, Pasadena, CA 91125.
- (l) Present address: Université de Genève, CH-1211, Geneva 4, Switzerland.
- (m) Present address: University of Illinois, Urbana, IL 61801.
- (n) Present address: CERN, CH-1211, Geneva 23, Switzerland.
- (o) Present address: University of Florida, Gainesville, FL 32611.
- ¹D. Karlen, Nucl. Phys. **B289**, 23 (1987); Ph.D. thesis, Stanford University, SLAC Report No. 325, 1988.
- ²E. Ma and J. Okada, Phys. Rev. Lett. **41**, 287 (1978); **41**, 1759(E) (1978); K. Gaemers, R. Gastmans, and F. Renard, Phys. Rev. D **19**, 1605 (1979); G. Barbiellini, B. Richter, and J. L. Siegrist, Phys. Lett. **106B**, 414 (1981); D. L. Burke, in *From the Planck Scale to the Weak Scale: Towards a Theory of the Universe*, proceedings of the Theoretical Advanced Study Institute in Particle Physics—TASI 86, Santa Cruz, California, 1986, edited by H. E. Haber (World Scientific, Singapore, 1987), pp. 497–540; M. Caffo, R. Gatto, and E. Remiddi, Nucl. Phys. **B286**, 293 (1987); M. Chen, C. Dionisi, M. Martinez, and X. Tata, Phys. Rep. **159**, 201 (1988).
- ³R. H. Schindler *et al.*, Phys. Rev. D **24**, 78 (1981); B. W. LeClaire, Ph.D. thesis, Stanford University, SLAC Report No. 321, 1987.
- ⁴F. A. Berends and R. Kleiss, Nucl. Phys. **B228**, 537 (1983).
- ⁵M. L. Perl *et al.*, Phys. Rev. D **34**, 3321 (1986).
- ⁶F. A. Berends and R. Kleiss, Nucl. Phys. **B186**, 22 (1981).